2019 American Control Conference (ACC)
Philadelphia, PA, USA, July 10-12, 2019

Decentralized Optimal Merging Control for Connected and Automated Vehicles

Wei Xiao and Christos G. Cassandras

Abstract— **This paper addresses the optimal control of Connected and Automated Vehicles (CAVs) arriving from two roads at a merging point where the objective is to jointly minimize the travel time and energy consumption of each CAV. The solution guarantees that a speed-dependent safety constraint is always satisfied, both at the merging point and everywhere within a control zone which precedes it. We first analyze the case of no active constraints and prove that under certain conditions the safety constraint remains inactive, thus significantly simplifying the determination of an explicit decentralized solution. Our analysis allows us to study the tradeoff between the two objective function components (travel time and energy within the control zone). Simulation examples are included to compare the performance of the optimal controller to a baseline with human-driven vehicles with results showing improvements.**

I. INTRODUCTION

Traffic management at merging points (usually, highway on-ramps) is one of the most challenging problems within a transportation system in terms of safety, congestion, and energy consumption, in addition to being a source of stress for many drivers [14], [15], [18]. Advancements in next generation transportation system technologies and the emergence of CAVs (also known as self-driving cars or autonomous vehicles) have the potential to drastically improve a transportation network's performance by better assisting drivers in making decisions, ultimately reducing energy consumption, air pollution, congestion and accidents. One of the very early efforts exploiting the benefit of CAVs was proposed in [5], where an optimal linear feedback regulator is introduced for the merging problem to control a single string of vehicles. An overview of automated intelligent vehicle-highway systems was provided in [16].

There has been significant research in assisted freeway merging offering guidance to drivers so as to avoid congestion and collisions. A Classification and Regression Tree (CART) method was used in [19] to model merging behavior and assist decisions in terms of the time-to-collision between vehicles. The Long Short-Term Memory (LSTM) network was used in [3] to predict possible long-term congestion. In [23], a Radial Basis Function-Artificial Neural Networks (RBF-ANN) is used to forcast the traffic volume in a merging area. However, such assisted merging methods do not take advantage of autonomous driving so as to possibly automate the merging process in a cooperative manner.

A number of centralized or decentralized merging control mechansims have been proposed [9], [2], [7], [8], [15], [12], [10], [13]. In the case of decentralized control, all computation is performed on board each vehicle and shared only with a small number of other vehicles which are affected by it. Optimal control problem formulations are used in some of these approaches, while Model Predictive Control (MPC) techniques are employed as an alternative, primarily to account for additional constraints and to compensate for disturbances by re-evaluating optimal actions. The objectives specified for optimal control problems may target the minimization of acceleration as in [12] or the maximization of passenger comfort (measured as the acceleration derivative or jerk) as in [9], [11]. MPC approaches have been used in [2], [8], as well as in [9] when inequality constraints are added to the originally considered optimal control problem. The Control Barrier Function (CBF) approach has also been considered in [21] with the same problem formulation as in this paper.

In [27], a decentralized optimal control framework is provided for a signal-free intersection. This may be viewed as a process of merging multiple traffic flows so that the highway merging problem is a special case. However, as detailed in the sequel, there are several differences in the formulation and analysis we pursue here in terms of the objective function and the safety constraints used.

In this paper, we develop a decentralized optimal control framework for each CAV approaching a merging point from one of two roads (often, a highway lane and an on-ramp lane). Our objective differs from formulations in [9], [12] or [27]; moreover, it is designed to guarantee that a hard speed-dependent safety constraint is always satisfied. In particular, our objective combines minimizing (i) the travel time of each CAV over a given road segment from a point entering a Control Zone (CZ) to the eventual Merging Point (MP) and (ii) a measure of its energy consumption. This allows us to explore the trade-off between these two metrics as a function of a weight factor. The problem incorporates CAV speed and acceleration constraints, and a hard safety constraint requiring a minimal headway between adjacent vehicles at all times as well as guaranteed collision avoidance at the MP. We derive an analytical solution of the problem and identify several properties of an optimal trajectory. This allows us to obtain simple to check conditions under which the safe distance constraint is guaranteed to not become active (which significantly reduces computation); in cases

This work was supported in part by NSF under grants ECCS-1509084 and CNS-1645681, by AFOSR under grant FA9550-12-1-0113, by ARPA-E's NEXTCAR program under grant DE-AR0000796, and by Bosch and the MathWorks.

The authors are with the Division of Systems Engineering and Center for Information and Systems Engineering, Boston University, Brookline, MA, 02446, USA {xiaowei,cgc}@bu.edu

where it does become active, we include constrained arcs as part of an optimal trajectory. Thus, we can identify when a trajectory exists that provably always satisfies all constraints and explicitly determine the optimal merging trajectory of each CAV.

The paper is structured as follows. In Section II, we present the merging process model and formulate the optimal merging control problem including all safety requirements that must be satisfied at all times. In Section III, the optimal solutions in all cases are presented. We include simulation examples and conclusions in Sections IV and V respectively.

II. PROBLEM FORMULATION

The merging problem arises when traffic must be joined from two different roads, usually associated with a main lane and a merging lane as shown in Fig.1. We consider the case where all traffic consists of CAVs randomly arriving at the two lanes joined at the Merging Point (MP) M where a collison may occur. The segment from the origin O or O' to the merging point M has a length L for both lanes, and is called the Control Zone (CZ). We assume that CAVs do not overtake each other in the CZ. A coordinator is associated with the MP whose function is to maintain a First-In-First-Out (FIFO) queue of CAVs based on their arrival time at the CZ and enable real-time communication with the CAVs that are in the CZ as well as the last one leaving the CZ. The FIFO assumption imposed so that CAVs cross the MP in their order of arrival is made for simplicity and often to ensure fairness, but can be relaxed through dynamic resequencing schemes, e.g., as described in [24].

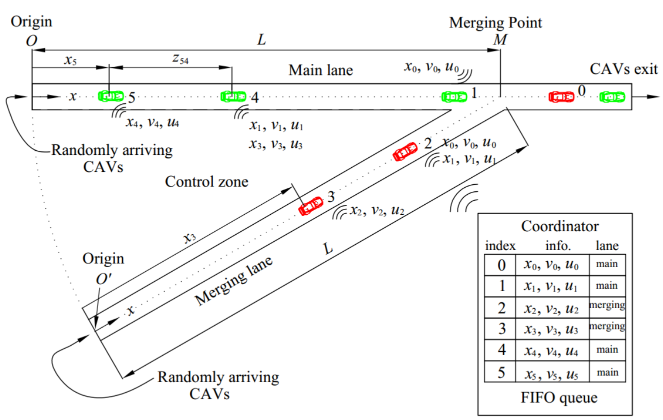

Fig. 1. The merging problem

Let $S(t)$ be the set of FIFO-ordered indices of all CAVs located in the CZ at time t along with the CAV (whose index is 0 as shown in Fig.1) that has just left the CZ. Let $N(t)$ be the cardinality of $S(t)$. Thus, if a CAV arrives at time t it is assigned the index $N(t)$. All CAV indices in $S(t)$ decrease by one when a CAV passes over the MP and the vehicle whose index is -1 is dropped.

The vehicle dynamics for each CAV $i \in S(t)$ along the lane to which it belongs take the form

$$\begin{bmatrix} \dot{x}_i(t) \\ \dot{v}_i(t) \end{bmatrix} = \begin{bmatrix} v_i(t) \\ u_i(t) \end{bmatrix} \tag{1}$$

where $x_i(t)$ denotes the distance to the origin O (O') along the main (merging) lane if the vehicle i is located in the main (merging) lane, $v_i(t)$ denotes the velocity, and $u_i(t)$ denotes the control input (acceleration). We consider two objectives for each CAV subject to three constraints, as detailed next.

Objective1 (Minimizing travel time): Let t_i^0 and t_i^m denote the time that CAV $i \in S(t)$ arrives at the origin O or O' and the merging point M, respectively. We wish to minimize the travel time $t_i^m - t_i^0$ for CAV i.

Objective2 (Minimizing energy consumption): We also wish to minimize energy consumption for each CAV $i \in S(t)$ expressed as

$$J_i(t_i^m, u_i(t)) = \int_{t_i^0}^{t_i^m} C_i(u_i(t))dt, \tag{2}$$

where $C_i(\cdot)$ is a strictly increasing function of its argument.

Constraint1 (Safety constraints): Let i_p denote the index of the CAV which physically immediately precedes i in the CZ (if one is present). We require that the distance $z_{i,i_p}(t) := x_{i_p}(t) - x_i(t)$ be constrained by the speed $v_i(t)$ of CAV $i \in S(t)$ so that

$$z_{i,i_p}(t) \geq \varphi v_i(t) + \delta, \quad \forall t \in [t_i^0, t_i^m], \tag{3}$$

where φ denotes the reaction time (as a rule, $\varphi = 1.8$ is used, e.g., [17]). If we define z_{i,i_p} to be the distance from the center of CAV i to the center of CAV i_p, then δ is a constant determined by the length of these two CAVs (generally dependent on i and i_p but taken to be a constant over all CAVs for simplicity).

Constraint2 (Safe merging): There should be enough safe space at the MP M for a merging CAV to cut in, i.e.,

$$z_{1,0}(t_1^m) \geq \varphi v_1(t_1^m) + \delta. \tag{4}$$

Constraint3 (Vehicle limitations): Finally, there are constraints on the speed and acceleration for each $i \in S(t)$:

$$\begin{aligned} v_{min} &\leq v_i(t) \leq v_{max}, \forall t \in [t_i^0, t_i^m], \\ u_{min} &\leq u_i(t) \leq u_{max}, \forall t \in [t_i^0, t_i^m], \end{aligned} \tag{5}$$

where $v_{max} > 0$ and $v_{min} \geq 0$ denote the maximum and minimum speed allowed in the CZ, while $u_{min} < 0$ and $u_{max} > 0$ denote the minimum and maximum control input, respectively.

Problem Formulation. Our goal is to determine a control law to achieve objectives 1-2 subject to constraints 1-3 for each $i \in S(t)$ governed by the dynamics (1). Choosing $C_i(u_i(t)) = \frac{1}{2}u_i^2(t)$ in (2) and combining objectives 1 and 2, we formulate the following optimal control problem for each CAV:

$$\min_{u_i(t)} J_i(t_i^m, u_i(t)) := \beta(t_i^m - t_i^0) + \int_{t_i^0}^{t_i^m} \frac{1}{2}u_i^2(t)dt, \tag{6}$$

subject to (1), (3), (4), (5), the initial and terminal position conditions $x_i(t_i^0) = 0$, $x_i(t_i^m) = L$, and given t_i^0, v_i^0 (where

v_i^0 denotes the initial speed). The weight factor $\beta \geq 0$ can be adjusted to penalize travel time relative to the energy cost. The two terms in (6) need to be properly normalized. Thus, by using $\alpha \in [0,1]$, we construct a convex combination as follows:

$$\begin{aligned} J_i(t_i^m, u_i(t)) &= \int_{t_i^0}^{t_i^m} \beta + \frac{1}{2}u_i^2(t)dt \\ &= \int_{t_i^0}^{t_i^m} \alpha + \frac{\frac{1}{2}(1-\alpha)\frac{1}{2}u_i^2(t)}{\frac{1}{2}\max\{u_{max}^2, u_{min}^2\}}dt \end{aligned} \tag{7}$$

where $\beta = \frac{\alpha \max\{u_{max}^2, u_{min}^2\}}{2(1-\alpha)}$ and use (6) as the problem to be solved.

III. DECENTRALIZED FRAMEWORK

Note that (6) can be locally solved by each CAV i provided that there is some information sharing with two other CAVs: CAV i_p which physically immediately precedes i and is needed in (3) and CAV $i-1$ so that i can determine whether this CAV is located in the same lane or not. With this information, CAV i can determine which of two possible cases applies: (i) $i_p = i-1$, i.e., i_p is the CAV immediately preceding i in the FIFO queue (e.g., CAVs 3 and 5 in Fig.1), and (ii) $i_p < i-1$, which implies that CAV $i-1$ is in a different lane from i (e.g., CAVs 2 and 4 in Fig.1). It is now clear that we can solve problem (6) for any $i \in S(t)$ in a decentralized way in the sense that CAV i needs only its own local information and information from $i-1$, as well as from i_p in case (ii). Observe that if $i_p = i-1$, then (4) is a redundant constraint; otherwise, we need to separately consider (3) and (4). Therefore, we will analyze each of these two cases in what follows.

Assumption 1: The safety constraint (3), control and state constraints (5) are not active at t_i^0.

Since CAVs arrive randomly, there are two ways to handle violations of Assumption 1: (i) By ensuring that it holds through a Feasibility Enforcement Zone (FEZ) as in [26] which applies the necessary control prior to the CZ so as to enforce (3) and (5) upon arrival at the CZ, (ii) by foregoing optimality and simply controlling a CAV that violates Assumption 1 until all constraints become feasible within the CZ.

Under Assumption 1, we will start by analyzing the case of no active constraints and then study what happens as different constraints become active. In this paper, we limit ourselves to cases where (3) may become active which are much more challenging than (5); the latter can also be handled through an analysis similar to that found in [6].

A. *Unconstrained Optimal Control when $i-1 = i_p$*

Let $\mathcal{X}_i(t) := (x_i(t), v_i(t))$ be the state vector and $\boldsymbol{\lambda}_i(t) := (\lambda_i^x(t), \lambda_i^v(t))$ be the costate vector (for simplicity, in the sequel we omit explicit time dependence when no ambiguity arises). The Hamiltonian with the state constraint, control constraint and safety constraint adjoined is

$$\begin{aligned} H_i(\mathcal{X}_i, \boldsymbol{\lambda}_i, u_i) =& \frac{1}{2}u_i^2 + \lambda_i^x v_i + \lambda_i^v u_i \\ &+ \mu_i^a(u_i - u_{max}) + \mu_i^b(u_{min} - u_i) \\ &+ \mu_i^c(v_i - v_{max}) + \mu_i^d(v_{min} - v_i) \\ &+ \mu_i^e(x_i + \varphi v_i + \delta - x_{i_p}) + \beta \end{aligned} \tag{8}$$

The Lagrange multipliers $\mu_i^a, \mu_i^b, \mu_i^c, \mu_i^d, \mu_i^e$ are positive when the constraints are active and become 0 when the constraints are strict. Note that when the safety constraint (3) becomes active, the expression above involves $x_{i_p}(t)$ in the last term. When $i=1$, the optimal trajectory is obtained without this term, since (3) is inactive over all $[t_1^0, t_1^m]$. Thus, once the solution for $i=1$ is obtained (based on the analysis that follows), x_1^* is a given function of time and available to $i=2$. Based on this information, the optimal trajectory of $i=2$ is obtained. Similarly, all subsequent optimal trajectories for $i>2$ can be recursively obtained based on $x_{i_p}^*(t)$ with $i_p = i-1$.

Since $\psi_{i,1} := x_i(t_i^m) - L = 0$ is not an explicit function of time, the transversality condition [1] is

$$H_i(\mathcal{X}_i(t), \boldsymbol{\lambda}_i(t), u_i(t))|_{t=t_i^m} = 0 \tag{9}$$

with the costate boundary condition $\boldsymbol{\lambda}_i(t_i^m) = [(\nu_{i,1}\frac{\partial \psi_{i,1}}{\partial \mathcal{X}_i})^T]_{t=t_i^m}$, where $\nu_{i,1}$ denotes a Lagrange multiplier.

The Euler-Lagrange equations become

$$\dot{\lambda}_i^x = -\frac{\partial H_i}{\partial x_i} = -\mu_i^e \tag{10}$$

and

$$\dot{\lambda}_i^v = -\frac{\partial H_i}{\partial v_i} = -\lambda_i^x - \mu_i^c + \mu_i^d - \varphi\mu_i^e, \tag{11}$$

and the necessary condition for optimality is

$$\frac{\partial H_i}{\partial u_i} = u_i + \lambda_i^v + \mu_i^a - \mu_i^b = 0. \tag{12}$$

In this case, $\mu_i^a = \mu_i^b = \mu_i^c = \mu_i^d = \mu_i^e = 0$. Applying (12), the optimal control input is given by

$$u_i + \lambda_i^v = 0. \tag{13}$$

and the Euler-Lagrange equation (11) yields

$$\dot{\lambda}_i^v = -\lambda_i^x. \tag{14}$$

Therefore, (10) implies $\lambda_i^x(t) = a_i$, hence $\lambda_i^v(t) = -(a_i t + b_i)$, where a_i and b_i are integration constants. Consequently, we obtain the following optimal solution:

$$u_i^*(t) = a_i t + b_i \tag{15}$$

$$v_i^*(t) = \frac{1}{2}a_i t^2 + b_i t + c_i \tag{16}$$

$$x_i^*(t) = \frac{1}{6}a_i t^3 + \frac{1}{2}b_i t^2 + c_i t + d_i \tag{17}$$

where c_i and d_i are also integration constants. In addition, we have the initial conditions $x_i(t_i^0) = 0, v_i(t_i^0) = v_i^0$ and the terminal condition $x_i(t_i^m) = L$. The costate boundary conditions and (12) offer us $u_i(t_i^m) = -\lambda_i^v(t_i^m) = 0$ and

$\boldsymbol{\lambda}_i(t_i^m) = (a_i, 0)$, therefore, the transversality condition (9) gives us an additional relationship:

$$\beta + a_i v_i(t_i^m) = 0. \tag{18}$$

Then, for each $i \in S(t)$, we need to solve the following five nonlinear algebraic equations for a_i, b_i, c_i, d_i and t_i^m:

$$\begin{aligned}
&\frac{1}{2}a_i \cdot (t_i^0)^2 + b_i t_i^0 + c_i = v_i^0,\\
&\frac{1}{6}a_i \cdot (t_i^0)^3 + \frac{1}{2}b_i \cdot (t_i^0)^2 + c_i t_i^0 + d_i = 0,\\
&\frac{1}{6}a_i \cdot (t_i^m)^3 + \frac{1}{2}b_i \cdot (t_i^m)^2 + c_i t_i^m + d_i = L,\\
&a_i t_i^m + b_i = 0,\\
&\beta + \frac{1}{2}a_i^2 \cdot (t_i^m)^2 + a_i b_i t_i^m + a_i c_i = 0.
\end{aligned} \tag{19}$$

There may be four, six or eight solutions if we solve (19), depending on the values of t_i^0, β, L and v_i^0, but only one of the solutions is valid, i.e., it satisfies $t_i^m > t_i^0$ and t_i^m is a real number. The remaining solutions are either imaginary or negative numbers. The following six lemmas provide a number of useful properties of the optimal solution (15)-(17). The proofs of the lemmas are omitted due to space constraints but can be found in [22].

Lemma 1: The optimal terminal time t_i^m can be expressed as a polynomial equation in the known parameters t_i^0, β, L and v_i^0.

Lemma 2: The solution for a_i in (19) is independent of t_i^0. Moreover, $a_i \leq 0$.

Lemma 3: Given β, L and under optimal control (15) for $i, j \in S(t)$, if $v_i^0 = v_j^0$, then $t_i^m - t_j^m = t_i^0 - t_j^0$.

Lemma 4: Under optimal control (15), $v_i(t_i^m) = -\frac{\beta}{a_i}$ for all $i \in S(t)$, and $v_i(t)$ is strictly increasing for all $t \in [t_i^0, t_i^m]$ taking its maximum value at $t = t_i^m$ when $\beta > 0$. Moreover, $\lim_{\beta\to 0} \frac{\beta}{-a_i} = v_i^0$ and $\lim_{\beta\to 0} \frac{3a_i L}{a_i v_i^0 - 2\beta} = \lim_{\beta\to 0} \frac{3L}{v_i^0 + 2v_i(t_i^m)} = \frac{L}{v_i^0}$.

Lemma 5: Under optimal control (15), the travel time for $i \in S(t)$ satisfies $t_i^m - t_i^0 \leq \frac{L}{v_i^0}$.

Lemma 6: For two vehicles $i, j \in S(t)$ under optimal control (15), if $v_i^0 < v_j^0$ and $\beta > 0$, then $v_i(t_i^m) < v_j(t_j^m)$, $t_i^m - t_i^0 > t_j^m - t_j^0$ and $a_i < a_j < 0$.

Using Lemmas 1-6, we can establish Theorem 1 identifying conditions such that the safety constraint (3) is never violated for all $t \in [t_i^0, t_i^m]$ in an optimal trajectory. The proof of Theorem 1 can be found in [22]. The following assumption requires that if the arrival times of two CAVs are too close to each other, then the first one maintains its optimal terminal speed past the MP until the second one crosses it as well. This is to ensure that the first vehicle does not suddenly decelerate and cause the safety constraint to be violated during the last segment of the first vehicle's optimal trajectory.

Assumption 2: For a given constant $\zeta > \varphi$, any CAV $i-1 \in S(t)$ such that $t_i^0 - t_{i-1}^0 < \zeta$ maintains a constant speed $v_{i-1}(t) = v_{i-1}^*(t_{i-1}^m)$ for all $t \in [t_{i-1}^m, t_i^m]$.

Theorem 1: Under Assumptions 1-2, if CAVs i and i_p satisfy $v_i^0 \leq v_{i_p}^0$ and $t_i^0 - t_{ip}^0 \geq \varphi + \frac{\delta}{v_i^0}$, then, under optimal control (15), $z_{i,i_p}(t) \geq \varphi v_i(t) + \delta$ for all $t \in [t_i^0, t_i^m]$. Moreover, if $\beta > 0$, then $z_{i,i_p}(t) > \varphi v_i(t) + \delta$ for all $t \in [t_i^0, t_i^m]$.

Remark 1: The significance of Theorem 1 is in ensuring that the safety constraint (3) is strict for all $t \in [t_i^0, t_i^m]$ when $\beta > 0$, $v_i^0 \leq v_{i_p}^0$, $t_i^0 - t_{ip}^0 \geq \varphi + \frac{\delta}{v_i^0}$ and the optimal control (15) is applied to i and i_p. Therefore, in this case we do not need to consider the safety constraint throughout the optimal trajectory which significantly reduces computation.

B. Unconstrained Optimal Control when $i - 1 > i_p$

In this case, CAV i_p which physically precedes $i \in S(t)$ is different from $i-1$ which, therefore, is in a different lane than i. This implies that we need to consider the safe merging constraint (4) at $t = t_i^m$. We define a new state vector $\mathcal{X}_i(t) := (x_i(t), v_i(t))^T$. We also define a new terminal constraint $\psi_{i,2}(\mathcal{X}_i(t_i^m), t_i^m) := x_i(t_i^m) + \varphi v_i(t_i^m) + \delta - x_{i-1}(t_i^m) = 0$, where we have replaced the inequality in (4) by an equality in order to seek the most efficient safe merging possible and $x_{i-1}(t_i^m)$ is known (an explicit function of time).

Let $\boldsymbol{\psi}_i := (\psi_{i,1}, \psi_{i,2})^T$, $\boldsymbol{\nu}_i := (\nu_{i,1}, \nu_{i,2})^T$ and define the costate $\boldsymbol{\lambda}_i := (\lambda_i^x, \lambda_i^v)^T$. We can get the same Hamiltonian as in (8).

Since i is under unconstrained case, we have $\mu_i^a = \mu_i^b = \mu_i^c = \mu_i^d = \mu_i^e = 0$. Applying the optimality condition, we get the same results as (13)-(17). However, the transversality condition is explicitly written as

$$\beta + a_i v_i(t_i^m) - \frac{1}{2}u_i^2(t_i^m) + \frac{1}{\varphi}u_i(t_i^m)v_{i-1}(t_i^m) = 0 \tag{20}$$

By Assumption 2, it follows that at $t = t_i^m$ we have $v_{i-1}(t_i^m) = v_{i-1}(t_{i-1}^m)$, a constant known to CAV i, and $x_{i-1}(t_i^m) = v_{i-1}(t_{i-1}^m)(t_i^m - t_{i-1}^m)$ with t_{i-1}^m also known to CAV i. Then, for each $i \in S(t)$, we need to solve the following algebraic equations for a_i, b_i, c_i, d_i and t_i^m:

$$\begin{aligned}
&\frac{1}{2}a_i \cdot (t_i^0)^2 + b_i t_i^0 + c_i = v_i^0,\\
&\frac{1}{6}a_i \cdot (t_i^0)^3 + \frac{1}{2}b_i \cdot (t_i^0)^2 + c_i t_i^0 + d_i = 0,\\
&\frac{1}{6}a_i \cdot (t_i^m)^3 + \frac{1}{2}b_i \cdot (t_i^m)^2 + c_i t_i^m + d_i = L,\\
&v_{i-1}(t_{i-1}^m)(t_i^m - t_{i-1}^m) = \varphi(\frac{1}{2}a_i \cdot (t_i^m)^2 + b_i t_i^m + c_i) + \delta\\
&\beta + 0.5a_i^2 \cdot (t_i^m)^2 + a_i b_i t_i^m + a_i c_i - 0.5(a_i t_i^m + b_i)^2\\
&\qquad\qquad + \frac{1}{\varphi}(a_i t_i^m + b_i)v_{i-1}(t_{i-1}^m) = 0.
\end{aligned} \tag{21}$$

Observe that in this case there is no safety constraint involving CAVs i and $i-1$ for all $t \in [t_i^0, t_i^m)$ because they are in different lanes and only the safe merging constraint is of concern. Similar to Theorem 1, the following can be proved for $i-1$ and i:

Theorem 2: Under Assumptions 1-2, if CAVs i and $i-1$ satisfy $v_i^0 \leq v_{i-1}^0$ and $t_i^0 - t_{i-1}^0 \geq \varphi + \frac{\delta}{v_i^0}$, then, under optimal control (15) for both CAVs, the safe merging constraint (4) is satisfied.

Remark 2: Theorem 2 is useful when CAV i arrives much later than $i-1$, i.e., $t_i^0 >> t_{i-1}^0$. In this case, if we use the optimal control solved by (21), one or more of the constraints in (5) will most probably be violated. If Theorem 2 does not apply, we can also use (15) for i and check whether the safe merging constraint (4) is satisfied or not. If it is, then the solution is complete; otherwise, we use the optimal control obtained through (21).

In contrast, when these conditions in Theorem 1 or 2 are not satisfied, we need to consider the possibility of constrained arcs such that $z_{i,i_p}(t) = \varphi v_i(t)+\delta$ on the optimal trajectory. This case is discussed next.

C. Safety Constraint Active

The unconstrained optimal controllers in Sec. III-A and Sec. III-B can offer an optimal reference for the MPC controller [8] or CBF controller [21]. We can also solve the constrained case with the optimal control method, as discussed next.

Suppose the safety constraint (3) becomes active on an optimal trajectory at some time $t_1 \in (t_i^0, t_i^m]$ (where t_1 will be optimally determined), clearly, if the original unconstrained optimal trajectory obtained through (15), (16), (17) and (18) violates (3) at any $t \in [t_i^0, t_i^m]$ with t_i^m evaluated through (18), then *a new optimal trajectory needs to be derived over the entire interval* $[t_i^0, t_i^m]$. This is done by decomposing this trajectory into an initial segment $[t_i^0, t_1)$ (where t_1 is to be determined as part of the optimization process) followed by an arc where (3) is active. The detailed process for obtaining a complete optimal solution is given in [22].

If an exit point t_2 exists in the case $i-1 = i_p$, we can find the constrained optimal solution as detailed in [22]. In the case $i-1 > i_p$, we can always find an exit time t_2 from the safety constrained arc on an optimal trajectory since the safe merging constraint between i and $i-1$ should be satisfied at t_i^m. If a feasible solution for t_2 is determined, it is possible that the safety constraint (3) becomes active again at some $t_3 \in [t_2, t_i^m]$. Thus, we use the same method to deal with the construction of a complete optimal trajectory recursively.

IV. SIMULATION EXAMPLES

We have used the Vissim microscopic multi-model traffic flow simulation tool as a baseline to compare with the optimal control approach we have developed. The car following model in Vissim is based on [20] and simulates human psycho-physiological driving behavior.

The simulation parameters used are as follows: $L = 400m$, $\varphi = 1.8$, $\delta = 0$, $v_{max} = 30m/s$, $v_{min} = 10m/s$, $u_{max} = 3.924m/s^2$ and $u_{min} = -5.886m/s^2$. The simulation under optimal control is conducted in MATLAB by using the same arrival process input and initial conditions as in Vissim. The CAVs arrive randomly with a rate of 600 CAVs per hour for both lanes. The MATLAB computation time for the unconstrained cases in Sec. III-A and Sec. III-B is about 1 second (Intel(R) Core(TM) i7-8700 CPU @ 3.2GHz 3.2GHz), while the constrained optimal solution computation time ranges from 3 seconds to 30 seconds, depending on whether i_p is under recursively constrained optimal control.

We limit ourselves here to an example where the safety constraint becomes active for a case with $i_p = i-1$, $t_{i_p}^0 = 0s$, $v_{i_p}^0 = 20m/s$, $t_i^0 = 2.7s$, $v_i^0 = 27m/s$, $\beta = 2.667$ ($\alpha = 0.26$) (additional examples can be found in [22]. We apply the optimal controller derived in Sec. III-C. The optimal value of the constraint arc entry point t_1 is determined to be $t_1^* = 9.25s$ and an exit point $t_2^* = 15.76s$ does exist. The new optimal control and trajectory are shown in Figs. 2-3.

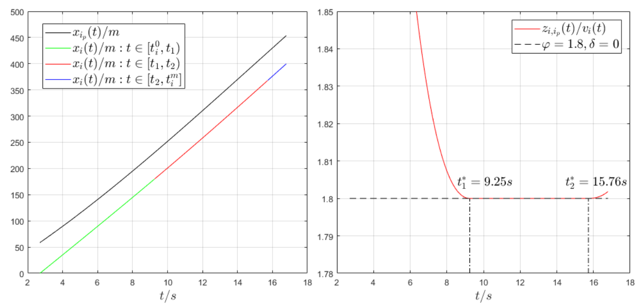

Fig. 2. The position and safety constraint profiles for the vehicles i and i_p under constrained optimal control with entry point t_1 and exit point t_2.

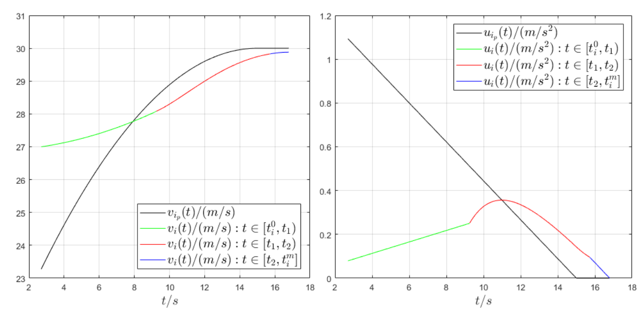

Fig. 3. The speed and control input profiles for the vehicles i and i_p under constrained optimal control with entry point t_1 and exit point t_2.

The simulation results regarding the performance of optimal control under two example trade-off parameters compared to that in Vissim are summarized in Table I. We can see that the objective function defined in (6) is significantly improved under optimal control compared to the Vissim simulation for both cases ($\alpha = 0.26$ and $\alpha = 0.41$). The same applies to the average travel times.

Recognizing that $\frac{1}{2}u^2(t)$ is only an approximation of the actual fuel consumption of a vehicle, we have used the polynomial metamodel proposed in [4] for a more accurate evaluation of fuel consumption as a function of both $v_i(t)$ and acceleration $u_i(t)$. This model is defined as $\dot{f}_v(t) = \dot{f}_{cruise}(t) + \dot{f}_{accel}(t)$ where $\dot{f}_{cruise}(t) = \omega_0 + \omega_1 v_i(t) + \omega_2 v_i^2(t) + \omega_3 v_i^3(t)$, $\dot{f}_{accel}(t) = (r_0 + r_1 v_i(t) + r_2 v_i^2(t))u_i(t)$ where ω_0, ω_1, ω_2, ω_3, r_0, r_1 and r_2 are positive coefficients (we used the values reported in [4]). It is assumed that during braking with $u_i(t) < 0$ no fuel is consumed. The average fuel consumptions are $48.6124mL$ and $68.3194mL$ under

TABLE I

OBJECTIVE FUNCTION COMPARISON

Items	OC		Vissim	
Weight	α=0.26	α=0.41	α=0.26	α=0.41
Ave. time (s)	17.1989	15.3132	25.0813	
Main time (s)	17.2109	15.3261	17.9935	
Merg. time (s)	17.1867	15.3000	32.3267	
Ave. $\frac{1}{2}u_i^2(t)$	4.9517	10.7603	20.0918	
Main $\frac{1}{2}u_i^2(t)$	4.9027	10.6644	9.4066	
Merg. $\frac{1}{2}u_i^2(t)$	5.0018	10.8583	31.0144	
Ave. obj.	38.0965	54.6923	65.0807	91.0385
Main obj.	38.0842	54.6765	42.9839	62.3554
Merg. obj.	38.1091	54.7085	87.6687	120.3539

optimal control when $\alpha = 0.26$ and $\alpha = 0.41$, respectively, and the average fuel consumption in Vissim is $36.9954mL$. As is to be expected, fuel consumption under optimal control is larger compared to that obtained in the Vissim simulation, since the form used for the objective function in (6) is different from the one in [4]. It remains unclear what an accurate fuel consumption model is and this is the subject of ongoing work aiming at appropriate modifications of (6).

V. CONCLUSIONS

We have derived a decentralized optimal control solution for the traffic merging problem that jointly minimizes the travel time and energy consumption of each CAV and guarantees that a speed-dependent safety constraint is always satisfied. Under certain simple-to-check condition in Theorems 1,3, we have shown that the safety constraint remains inactive and computation is simplified. Otherwise, we can still derive a complete solution that may include one or more arcs where the safety constraint is active. We have not taken into account speed and acceleration constraints for each CAV, which will be incorporated in future work by including appropriate arcs in the optimal trajectory as in [27]. Ongoing research is exploring the use of approximate solutions (e.g., the use of control barrier functions) as an alternative to an optimal control solution if the latter becomes computationally burdensome or if the use of more complex objective functions or more elaborate vehicle dynamics makes an optimal control approach prohibitive. Lastly, we will investigate the case where only a fraction of the traffic consists of CAVs, similar to the study in [25].

REFERENCES

[1] Bryson and Ho. *Applied Optimal Control*. Ginn Blaisdell, Waltham, MA, 1969.

[2] W. Cao, M. Mukai, and T. Kawabe. Cooperative vehicle path generation during merging using model predictive control with real-time optimization. *Control Engineering Practice*, 34:98–105, 2015.

[3] W. Chen, Z. Zhao, Z. liu, and Peter C. Y. Chen. A novel assistive on-ramp merging control system for dense traffic management. In *Proc. IEEE Conference on Industrial Electronics and Applications*, pp. 386–390, Siem Reap, 2017.

[4] M. Kamal, M. Mukai, J. Murata, and T. Kawabe. Model predictive control of vehicles on urban roads for improved fuel economy. *IEEE Transactions on Control Systems Technology*, 21(3):831–841, 2013.

[5] W. Levine and M. Athans. On the optimal error regulation of a string of moving vehicles. *IEEE Transactions on Automatic Control*, 11(13):355–361, 1966.

[6] A. A. Malikopoulos, C. G. Cassandras, and Yue J. Zhang. A decentralized energy-optimal control framework for connected and automated vehicles at signal-free intersections. *Automatica*, 2018(93):244–256, 2018.

[7] V. Milanes, J. Godoy, J. Villagra, and J. Perez. Automated on-ramp merging system for congested traffic situations. *IEEE Transactions on Intelligent Transportation Systems*, 12(2):500–508, 2012.

[8] M. Mukai, H. Natori, and M. Fujita. Model predictive control with a mixed integer programming for merging path generation on motor way. In *Proc. IEEE Conference on Control Technology and Applications*, pp. 2214–2219, Mauna Lani, 2017.

[9] I. A. Ntousakis, I. K. Nikolos, and M. Papageorgiou. Optimal vehicle trajectory planning in the context of cooperative merging on highways. *Transportation Research*, 71, Part C:464–488, 2016.

[10] G. Raravi, V. Shingde, K. Ramamritham, and J. Bharadia. *Merge algorithms for intelligent vehicles. In: Sampath, P., Ramesh, S. (Eds.), Next Generation Design and Verification Methodologies for Distributed Embedded Control Systems*. Springer, Waltham, MA, 2007.

[11] C. Rathgeber, F. Winkler, X. Kang, and S. Muller. Optimal trajectories for highly automated driving. *International Journal of Mechanical, Aerospace, Industrial, Mechatronic and Manufacturing Engineering*, 9(6):946–952, 2015.

[12] J. Rios-Torres, A.A. Malikopoulos, and P. Pisu. Online optimal control of connected vehicles for efficient traffic flow at merging roads. In *Proc. IEEE 18th International Conference on Intelligent Transportation Systems*, pp. 2432–2437, Las Palmas, Spain, 2015.

[13] R. Scarinci and B. Heydecker. Control concepts for facilitating motorway on-ramp merging using intelligent vehicles. *Transport Reviews*, 34(6):775–797, 2014.

[14] B. Schrank, B. Eisele, T. Lomax, and J. Bak. The 2015 urban mobility scorecard. Texas A&M Transportation Institute, 2015.

[15] M. Tideman, M.C. van der Voort, B. van Arem, and F. Tillema. A review of lateral driver support systems. In *Proc. IEEE Intelligent Transportation Systems Conference*, pp. 992–999, Seatle, 2007.

[16] P. Varaiya. Smart cars on smart roads: problems of control. *IEEE Transactions on Automatic Control*, 38(2):195–207, 1993.

[17] K. Vogel. A comparison of headway and time to collision as safety indicators. *Accident Analysis & Prevention*, 35(3):427–433, 2003.

[18] D. De Waard, C. Dijksterhuis, and K. A. Broohuis. Merging into heavy motorway traffic by young and elderly drivers. *Accident Analysis and Prevention*, 41(3):588–597, 2009.

[19] J. Weng, S. Xue, and X. Yan. Modeling vehicle merging behavior in work zone merging areas during the merging inplementation period. *IEEE Transactions on Intelligent Transportation Systems*, 17(4):917–925, 2016.

[20] R. Wiedemann. Simulation des straenverkehrsflusses. In *Proc. of the Schriftenreihe des tnstituts fir Verkehrswesen der Universitiit Karlsruhe (In German language)*, 1974.

[21] Wei Xiao, Calin Belta, and Christos G. Cassandras. Decentralized merging control in traffic networks: A control barrier function approach. In *Proc. ACM/IEEE International Conference on Cyber-Physical Systems*, 2019. To appear.

[22] Wei Xiao and Christos G. Cassandras. Decentralized optimal merging control for connected and automated vehicles. *preprint arXiv:1809.07916*, 2018.

[23] X. Zang. The short-term traffic volume forecasting for urban interchange based on rbf artificial neural networks. In *Proc. IEEE Conference on Mechatronics and Automation*, pp. 2607–2611, Changchun, 2009.

[24] Yue J. Zhang and C. G. Cassandras. A decentralized optimal control framework for connected automated vehicles at urban intersections with dynamic resequencing. In *Proc. 57th IEEE Conference on Decision and Control*, pp. 217–222, Miami, 2018.

[25] Yue J. Zhang and C. G. Cassandras. The penetration effect of connected automated vehicles in urban traffic: an energy impact study. In *Proc. 2018 IEEE Conference on Control Technology and Applications*, pp. 620–625, Copenhagen, Denmark, 2018.

[26] Yue J. Zhang, C. G. Cassandras, and A. A. Malikopoulos. Optimal control of connected and automated vehicles at urban traffic intersections: A feasibility enforcement analysis. In *Proc. of the American Control Conference*, pp. 3548–3553, Seattle, 2017.

[27] Yue J. Zhang, A. A. Malikopoulos, and C. G. Cassandras. Optimal control and coordination of connected and automated vehicles at urban traffic intersections. In *Proc. of the American Control Conference*, pp. 6227–6232, Boston, 2016.